



# Optimizing E-Methanol Production: Effect of Electricity Price and Renewable Energy Volatility on Optimum Dimensioning and Operation

Jaakko Hyypää<sup>1,\*</sup> Hannu Karjunen<sup>1</sup> Nashmin Hosseinpour<sup>1</sup> Eero Inkeri<sup>1</sup> Tero Tynjälä<sup>1</sup>

<sup>1</sup> *Lappeenranta-Lahti University of Technology LUT, School of Energy Systems, Lappeenranta, Finland*

\*Corresponding author. Email: [Jaakko.Hyypia@lut.fi](mailto:Jaakko.Hyypia@lut.fi)

## ABSTRACT

Renewable energy can significantly reduce global CO<sub>2</sub> emissions, both directly by reducing the use of fossil-based energy sources and indirectly through power-to-X pathways. These pathways facilitate the production of various fuels and chemical feedstocks, offering alternatives to fossil-based products. This study focuses on optimizing e-methanol production chain to determine the most economically viable dimensioning of main process components and selection of operation strategy. The optimization task is executed with an open-source energy system modelling framework, considering different electricity supply alternatives, such as grid, wind power and combined wind and solar power. The analyzed system incorporates essential process components for hydrogen, methanol and CO<sub>2</sub> production, along with intermediate storages and alternative power supply profiles. The main finding of the study is that allowing flexible operation and over-dimensioning of the methanol synthesis plant, considerable, up to 46% cost savings can be achieved already in current market scheme. Moreover, the dynamic operation of the e-methanol plant may benefit electricity markets, by shifting demand to periods of electricity overproduction. The results of the study may be used in the planning of future investments, not only for individual plants but also for larger industrial clusters and energy infrastructure networks.

**Keywords:** *Power-to-methanol, PtX, methanol, hydrogen, electrolysis, synthesis, flexibility*

## 1. INTRODUCTION

The large-scale adoption of Variable Renewable Energy (VRE) production necessitates the development of Power to X-technologies (P2X) and e-fuels to facilitate the decarbonization of our societies. However, the variable nature of renewable power raises questions regarding the optimal design and operation of P2X process plants. Linking of the various production stages (electrolysis, synthesis) and feedstocks (carbon dioxide, hydrogen) in a timely fashion requires appropriately sized process components, storages and sophisticated prediction algorithms and operation guidelines.

Out of the numerous possible P2X chemical products e-methanol is selected as the final product in this work. Hank et al. and Sollai et. al [1], [2] summarise the reasons why e-methanol manufacturing holds great potential. An

industrial scale synthesis process is available, methanol has a large market (~100 Mt/year consumed) [3], high energy density and the possibility to act both as fuel and a platform molecule. Methanol is also relatively easy to store because it has a liquid form at normal conditions. Although methanol has a large market globally, e-methanol production is very small. This is mainly due to the poor cost competitiveness of e-methanol compared to traditional, fossil derived methanol, that can have production cost of between 100 to 250 USD per ton. [3].

Detailed studies about the e-methanol plant configurations, unit processes, and control strategies have been done previously. Sollai et al. [2] studied the technoeconomic feasibility of e-methanol production using surplus electricity production, based on detailed Aspen Plus model. Zheng et al. [4] studied optimal control strategies of e-methanol plant using electricity

market price data. Hank et al. [1] studied e-methanol production in Germany based on grid and wind supplied electricity. The results of these studies indicated that currently e-methanol production is not competitive compared to conventional e-methanol. The importance of electrolyser investment costs and the electricity costs for the final product cost are highlighted.

There are a lot of detailed studies that accurately describe the unit processes, but the electricity price and availability are assumed to be constant or are modelled based on correlation between full load hours and average electricity price. However, a system level optimization and main component sizing with different electricity availability and cost characteristic have not been extensively studied. This study utilizes values from previous studies to create a less detailed, general system model with a special focus on flexible operation, optimum capacity selection and the effects of different electricity supply options. Both electricity availability (VRE) and electricity cost are considered.

The primary objective is to minimize the cost of produced e-methanol by selecting suitable capacities for plant components, buffer storages and the implementation of suitable operational strategy on an hourly basis. For this optimization task and problem description, an open-source multi-scale energy systems modelling framework, Calliope, is utilized. Various electricity sources are considered, including grid electricity, wind power, solar power, and a combination of these. This study utilizes historical data spanning from 2018 to 2022 to describe the electricity supply options. Each year is treated as an independent case to study the variability of the solutions throughout the years. Electricity market spot prices and meteorological data for VRE production estimation is used for a location in South-Karelia, Finland. Investment costs of components and storages are estimated based on relevant literature. This study analyzes the volatility of the electricity price and renewable electricity production and its influence on optimum dimensioning.

Following research questions are answered:

- What is the techno-economical optimum sizing of e-methanol plant? How does the optimum sizing change when the electricity price and availability are changed?
- What is the most economical electricity supply option for e-methanol plant and how much the costs vary over several years?
- What kind of operation strategies are there for synthesis units, storages and electrolysers given the variable nature of renewable energy availability and fluctuating grid price?

These questions are essential for the generation of feasible P2X ecosystems that form complex

dependencies between the different sub-processes. Strongly coupled systems also require sophisticated modelling tools that can account for the variability and uncertainty of parameters, which is possible with our selected modelling tool.

The results indicate that the flexibility of the system is enabled by over dimensioning the electrolyser, although the exact sizing is dependent on assumed feedstock prices and generation profile, especially for the electricity supply. Thus, annual variations in wind and solar production profiles can therefore have a significant effect on the design of the system. From the perspective of the P2X plant operator, curtailment of renewable energy resulted in the least-cost production cost for methanol, but this might be in conflict with the global optimum of the whole energy system.

## 2. METHODOLOGY

The modelled e-methanol plant is in a single location, which leaves the need for analysing transport of materials outside of the scope of this research. Figure 1 illustrates the different process stages in the e-methanol production.

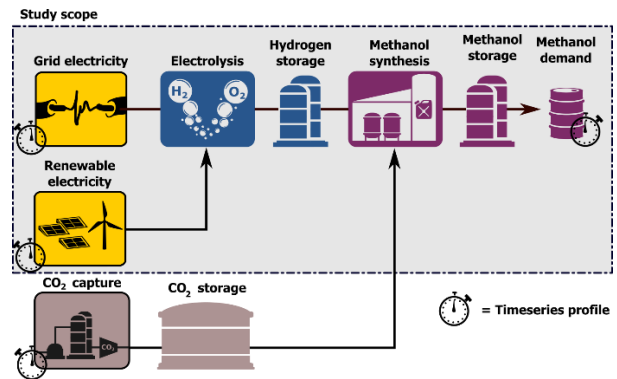


Figure 1. Simplified process diagram

A multiscale energy system modelling framework is used for describing the system and creating the optimization problem. Open-source software, Calliope, is used. [5] The used timestep resolution is 1 h. The linear optimization problem is solved with an open-source mixed integer program (MIP) solver, called CBC (COIN-OR Branch and Cut) [6]. However, for this problem, the problem is described as linear problem without integer decisions. The objective of the optimization is to find the minimum cost solution for the modelled system. The used objective function is described with Equation (1)

$$\min: z = \sum_{locations,techs} (cost_{loc,tech,k} \times weight_k) + \sum_{location,carrier,timestep} (unmet\_demand \times bigM) \quad (1)$$

where  $cost_{loc,tech,k}$  is the total cost of each technology in each location for cost class  $k$  and  $weight_k$  is the weight of cost class  $k$ . Here a value 1.0 is used and only monetary cost class is used [7]. The  $unmet\_demand$  variable is used to ensure feasibility of the optimization, together with a

large weight factor bigM. The results were inspected that no unmet demand exists in the result.

Figure 2 illustrates the different energy and material carriers and possible electricity supply options in the model. To scale the e-methanol plant, a component or a demand must be decided to set the production scale. In this work, the methanol demand is fixed to 100 MW or 18 tons per hour. The methanol storage between the methanol demand and the methanol synthesis plant decouples the methanol production from the demand, therefore allowing the synthesis plant to operate independently from the demand profile. The model matches the initial storage level to the storage level in the end of the simulation time, therefore ensuring that the energy balance of each storage over the simulation time equals zero.

Notice that some energy and material flows have been left outside the scope of this study. For example, the water required for electrolysis, and the heat and oxygen produced by the electrolysis are not studied. These auxiliary streams are neglected so the focus of the study can be better directed to the main process components.

## 2.1 Electricity Production Data

The production of solar photovoltaics and wind turbines is described at an hourly time resolution using a production potential timeseries. These timeseries describe the power per installed capacity for each technology at each timestep. Similarly, the grid electricity price is described at same resolution with a price timeseries. The study covers the years from 2018 to 2022, with each year studied separately. This method allows studying the effects of yearly variation of electricity production and price.

The photovoltaics production data for years 2018 – 2020 is produced with Photovoltaic Geographical Information System (PVGIS) [8]. The snow effects have not been considered.

The photovoltaics production data for 2021-2022 is not available on PVGIS. Therefore a different

methodology was used for this data. The ERA5 reanalysis database of the European Centre for Medium-Range Weather Forecasts (ECMWF) is used in this study to examine the performance of photovoltaic (PV) panels using Numerical Weather Prediction (NWP) data [9], [10]. Meteorological data such as shortwave radiation, temperature and 10 m wind components are retrieved from the ERA5 database, with a temporal resolution of one hour, in order to model the performance of photovoltaic panels.

The solar position with respect to the surface of the planet is one of the most significant characteristics to drive solar irradiance on the earth surface. To calculate the required solar angles like elevation angle and extract Direct Normal Irradiance (DNI) and Diffuse Horizontal Irradiance (DHI), Sandia National Laboratories' PVPerformance Modelling Collaborative (PVPMC) open-source tool is utilized [11].

The computation of the irradiance components on the Plane of Array—reflected ( $R_{POA}$ ), beam ( $B_{POA}$ ), and diffuse ( $D_{POA}$ )—is done by applying transposition model which requires computing Angle of Incidence (AOI) [12]. The Global POA irradiance ( $G_{POA}$ ) is obtained by adding them:

$$G_{POA} = B_{POA} + D_{POA} + R_{POA} \quad (2)$$

The Effective Irradiance ( $G_{eff}$ ) is driven by taking Incident Angle Reflection Losses into account on  $G_{POA}$  [13]. This is a crucial stage since it's necessary to take into consideration the real irradiance that photovoltaic modules will convert into electricity, which directly affects the final power output.

Finally, a PV power model based on the model by Huld et al. [14] is utilized to determine the power generation for crystalline silicon PV modules. An evaluation of the PV installation's potential for power generation is made possible by this model, which links the power output to the effective irradiance and module temperature. [14]

Module temperature for power model is calculated using the temperature and wind data from the ERA5

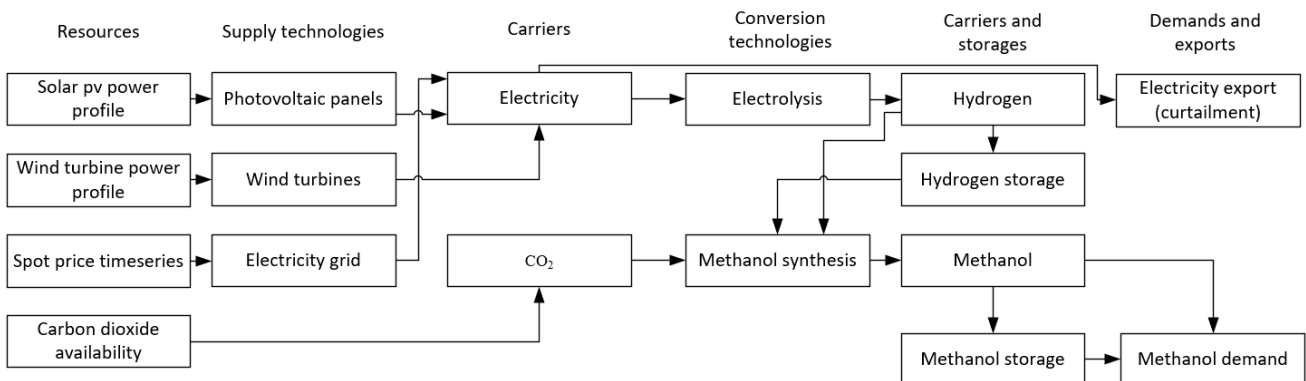


**Figure 2.** Energy and material carriers and different conversion and storage technologies simulated

dataset. The following empirical connection is employed for determining the module temperature ( $T_M$ ):

$$T_M = T_{amb} + \frac{G_{POA}}{U_0 + U_1 \cdot WS_M} \quad (3)$$

where, according to Koehl et al. [15],  $U_0$  and  $U_1$  are constants representing the heat transfer components specific to crystalline silicon (c-Si) PV modules.  $T_{amb}$  is the ambient temperature measured in 2 m.  $WS_M$  is wind speed obtained by wind components data.

The power generation results from the model and the reference data supplied by PVGIS exhibit an elevated level of correlation, as seen in the Figure 3.

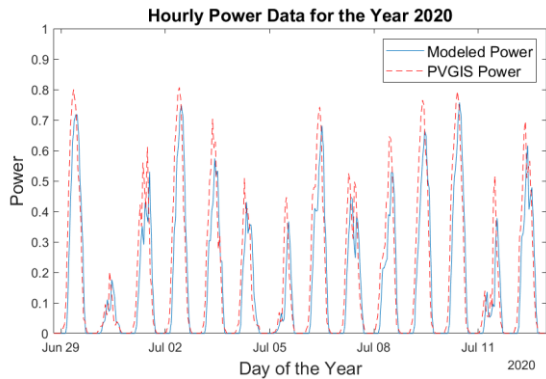


**Figure 3.** Correlation between Modeled Photovoltaic Power and PVGIS Power

Table 1 summarizes the key assumptions considering photovoltaics production data. The imaginary solar power plant is located in South Karelia, Finland, and the photovoltaics are installed in a fixed tilt and orientation installation.

**Table 1.** Photovoltaics production data

Solar radiation database	PVGIS-ERA5
Location	61.042, 28.459
Elevation	52 m
Slope	45 °
Azimuth	0 ° (South)
PV technology	Crystalline silicon
Full load hours	940 – 982 h

Wind turbine production data is also based on ERA5 data. [9], [10]. The ERA5 data has been previously applied for analyzing wind power production [16]–[18] and has shown to be reliable and applicable.

The wind velocity at an altitude of 100 m is taken and corrected to 125 m hub height with Equation (4).

$$v_2(z_2) = v_1(z_1) \cdot \frac{\ln(\frac{z_2}{z_0})}{\ln(\frac{z_1}{z_0})} \quad (4)$$

- where,  $v$  is velocity
- $z$  is height above ground level
- $z_0$  is surface roughness length, 0,5 is used for forest

A turbine-specific power coefficient factor ( $C_p$ ) is used to convert the theoretical power of the wind to the actual production of a wind turbine power with a diameter of 110m as described in Equation (5) [19].

$$P = \frac{1}{8} \cdot \rho \cdot D^2 \cdot \pi \cdot v^3 \cdot C_p \quad (5)$$

The power coefficient is estimated by taking the average of several turbine power coefficients from literature [20] in segments for different wind speeds ranging from 0 to 26 m/s. The data is smoothed by calculating a running average and then applying a smoothing spline fit for the power coefficients. Figure 4 illustrates the  $C_p$ -factor used for calculating turbine power. This timeseries is then divided by the maximum power of the turbine to create a relative power time series. This relative power time series is used as an input for the energy system modelling framework.

Table 2 summarizes the key parameters used to estimate the wind turbine power production. An imaginary wind farm with 3 MW turbines is assumed to be located in South Karelia, Finland with a hub height of 125 m above ground level. The annual full load hours of the turbine are quite modestly only around 2210 – 2770 h. Modern turbines with a larger diameter and higher hub height would likely reach much higher annual full load hours.

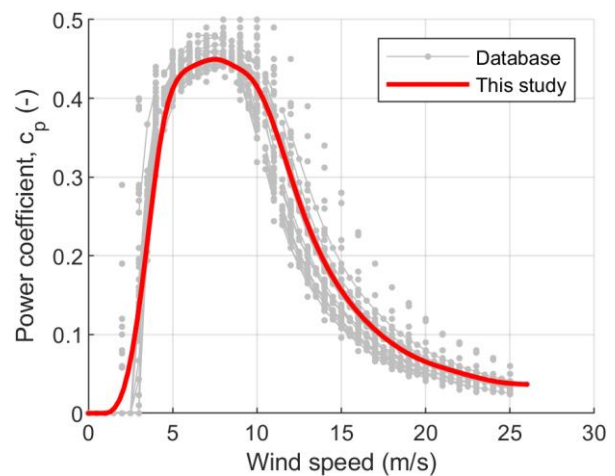


**Figure 4.**  $C_p$ -correlation used to calculate wind turbine power.

**Table 2.** Wind turbine production data

Weather data	ERA5
Location (WGS84)	61.003, 27.999
Wind speed altitude	100 m
Density of air	1,25 kg/m <sup>3</sup>
Corrected hub height	125 m
Rotor diameter	110 m
Nominal turbine size	3 MW

The grid electricity price is assumed to be the Nordpool day-head spot price for Finland. This data is acquired at one hour time resolution from ENSTO-E Transparency Platform [21]. No additional grid connection fees or transfer fees are included in the grid electricity cost.

The summary of different electricity supply alternatives on different years is shown in Table 3. The average grid electricity price has been increasing since 2020. At the same time the standard deviation of electricity price has also increased. The VRE production characteristics on the other hand are rather steady, with 2020 being exceptionally good wind production year. The full load hours of wind power are between 2210 and 2771 hours, while solar power has between 887 and 982 full load hours. The levelized cost of electricity for wind and solar power is calculated with capital recovery factor and the economical parameters described in chapter 2.1. The cost is between 59,4 €/MWh and 74,4 €/MWh for wind power. Solar power is slightly more expensive, cost ranging from 71,8 €/MWh to 79,4 €/MWh. The relatively high levelized cost of VRE is mainly due to high interest rate, 10 %, used.

**Table 3.** Characterization of the electricity source data

Year	2018	2019	2020	2021	2022
Grid electricity average price [€/MWh]	46.8	44.0	28.0	72.3	154.0
Grid electricity price standard deviation [€/MWh]	15.1	15.3	21.1	66.0	132.4
Wind power FLH [h]	2210	2410	2770	2440	2370
Wind power levelized cost [€/MWh]	74.4	68.3	59.5	67.6	69.3
Solar power FLH [h]	982	941	967	883	938
Solar power levelized cost [€/MWh]	71.8	74.9	73.1	79.9	75.2

## 2.2 Financial and Technical Parameters

The financial and technical parameters used in the model are summarized in Table 4. The parameters are estimated based on relevant literature. Levelised cost of methanol (LCOM) is calculated with Equation 6 [1]

$$\text{LCOM} = \frac{\text{Annuity (€)} + \text{Annual operational and variable cost (€)}}{\text{Annual production of MeOH (ton)}} \quad (6)$$

**Table 4.** Financial and technical data for different technologies

<b>Interest rate</b>		10 %
<b>Wind turbines, onshore</b> [22], [23]	Capex	1400 €/kW
	Lifetime	20 a
<b>Solar photovoltaics, fixed installation</b> [22], [23]	Capex	600 €/kW <sub>p</sub>
	Lifetime	20 a
<b>Electrolysis, alkaline</b> [23]–[25]	Efficiency	65 % (LHV)
	Capex	750 €/kW <sub>e</sub>
	Opex*	32,5€/kW <sub>e</sub> per year
	Lifetime	20 a
<b>Hydrogen storage, lined rock cavern</b>	Capex [26]	65 €/kg
	Lifetime	20 a
<b>Methanol synthesis</b> [2], [4]	Capex	800 €/kW <sub>MeOH</sub>
	Lifetime	20 a
	H <sub>2</sub> consumption	0,208 kg/kg <sub>MeOH</sub>
	CO <sub>2</sub> consumption	1,45 kg/kg <sub>MeOH</sub>
	Minimum part load	50 %
	Maximum ramping	10% per hour
<b>Methanol storage</b>	Capex	100 €/t
	Lifetime	20 a
<b>CO<sub>2</sub> supply</b>	Cost of CO <sub>2</sub>	100 €/t

\* The electrolyser opex is calculated based on the limited lifetime of the electrolyser stack. It is assumed that the stack must be replaced once in 10 years, and the stack cost is 50% of the total electrolyser investment. The cost is evenly distributed for every year in the form of opex.

### 3. RESULTS

Four different cases were studied. Case 1 is a reference scenario with grid electricity, where no flexible operation or storage capacity are allowed. Synthesis and electrolysis will be operated with a constant power that is determined by the methanol demand (100MW<sub>MeOH</sub>). Therefore, the average cost of used electricity will be the average electricity cost over the given year. Case 2 uses the same electricity cost data, but storage use, and part load operation are allowed. The operation profile and process capacities are optimized with the energy system modelling framework. Case 3 uses only wind power, and Case 4 uses both wind and solar power. For both VRE cases, the energy system modelling tool decides the optimum capacity of VRE production. Curtailment is allowed and no revenue from the curtailed electricity is assumed. Table 5 summarises the different cases considered in the study.

**Table 5.** Summary of studied cases

Case 1: <i>Grid, full load</i>	Grid electricity, always available, spot-price. No storage use allowed – operation on nominal capacity through the year
Case 2: <i>Grid, optimized</i>	Grid electricity, always available, spot-price. Storage use and part load operation allowed. Optimized to reach minimum cost
Case 3: <i>Wind only</i>	Wind power electricity, availability from timeseries. Storage use and part load operation allowed. Optimized to reach minimum cost
Case 4: <i>Wind + solar</i>	Wind and solar power electricity, availability from timeseries. Storage use and part load operation allowed. Optimized to reach minimum cost

#### 3.1 Levelized Cost of E-methanol

Figure 5 illustrates the calculated levelized cost of produced e-methanol for the different cases on different years. Both the lowest and highest cost was achieved with grid electricity – the lowest result was reached with *grid, optimized* case on year 2020, when average price of electricity was low, and the highest cost was achieved for *grid, full load* on year 2022, when no optimization was done, and plant was operated on full load throughout the year. At the same time 2022 showed exceptionally high electricity prices.

Using part load operation and storages always decreases the levelized cost, although the highest effects are seen in years 2021 and 2022, when the grid electricity price volatility was higher. In years 2018-2020 the

benefit of optimizing the system operation is small. For example, in 2018 the levelized cost decreased from 849 €/ton to 839 €/ton, whereas in 2022 the decrease is from 1992 €/ton to 1073 €/ton.

The levelized cost of e-methanol with cases that utilise VRE is higher than with optimized grid electricity use. Levelized cost in case *Wind only* is between 1331 €/ton and 1530 €/ton, while case *Grid, optimized* showed a cost between 614 €/ton and 1073 €/ton. Adding solar power, in case *Wind and solar*, decreases the levelized cost to between 1246 €/ton and 1411 €/ton. The levelized costs calculated in this study fall within the range of costs estimated by IRENA (2021) [3], which projected a levelized cost of green methanol to be between 700 and 1500 €/ton (USD/EUR rate 0.91). Additionally, Sollai et al. [2] provided an independent estimate, suggesting a cost of 960 €/ton for e-methanol.

However, this study did not consider electricity transmission and grid connection costs, that could make using locally produced VRE more economically competitive option. Additionally, the used interest rate, 10 %, was rather high and the full load hours of VRE were quite modest. All these factors increase the levelized cost of VRE, making it less competitive against grid electricity. A more detailed study including all the different costs associated with both electricity supply alternatives could answer to the relative cost competitiveness of VRE and grid electricity.

It is worth noting that even though VRE production is variable by nature, there is less variation in the levelized cost of e-methanol between different years, compared to production relying only on spot priced grid electricity.

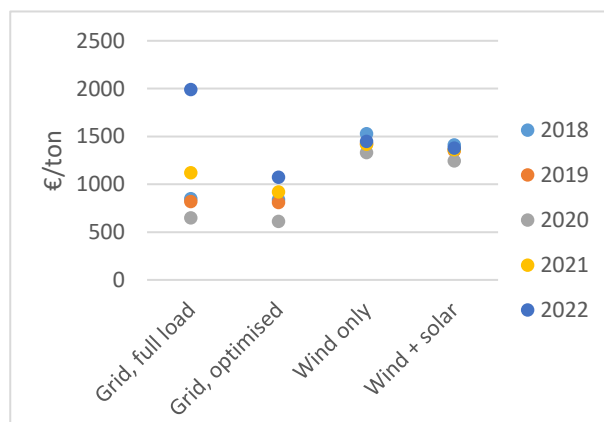


**Figure 5** Levelized cost of e-methanol for different cases.

#### 3.2 Component Capacities

The capacities of system components on different cases and different years are illustrated. Figure 6 shows the optimized relative electrolyser capacity and its variation through years. Relative electrolyser capacity is calculated by dividing the optimized electrolyser

capacity with the electrolyser capacity in case *Grid, full load*, where the electrolyser capacity is fixed.

The model utilized data from 2018 to 2022 and the spot price of electricity in Finnish grid has become increasingly volatile during this period. This has a large impact on the optimal operation of an e-methanol plant, if the electricity is acquired from the spot markets. For 2018 and 2019 the full load hours for optimized electrolyser capacity were at 7600 – 8100 hours (relative size 1,10 to 1,15), whereas in 2022 the optimum decreased to mere 2800 hours (relative size 3,13). The results show that if the electricity price is very volatile, it is more beneficial to considerably over dimension the electrolyser size and operate it only during the hours of low-cost electricity. This also increases the hydrogen storage size required. Effect is very clearly seen in optimum relative hydrogen storage size in Figure 7, that increases from less than 10 hours for year 2018 to 117 hours for year 2022.

Using both wind and solar power compared to wind only, decreases both the electrolyser capacity and the variation in the optimum electrolyser capacity. *Wind and solar* case has an optimum electrolyser relative capacity between 1.95 and 2.23 compared to 2,14 to 2,64 for *Wind only*.

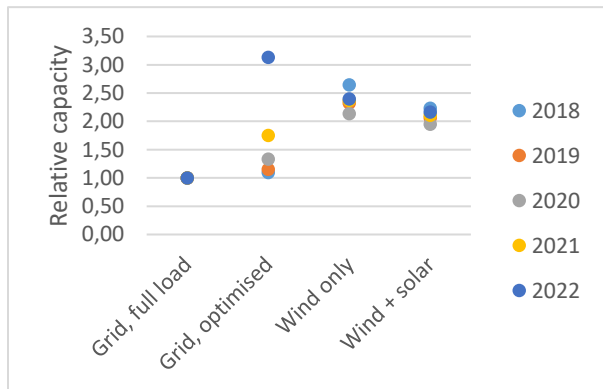


**Figure 6.** Relative electrolyser optimum capacity for different cases. Case 1 = 1,0.

The relative capacity of the hydrogen storage is plotted in Figure 7. Notice that case *grid, full load* has no hydrogen storage, therefore the value is zero. Hydrogen storage capacity in figure 6 describes the storage capacity relative to the electrolyser hydrogen production capacity.

Case *wind only* shows variations in storage size. Years 2018, 2019 and 2022 have optimum size of between 71 and 74 hours, but 2021 has 99 hours and 2020 152 hours. The year 2020 stands out also in Table 3 as having the highest full load hours for wind power. Optimum hydrogen storage size decreases to between 29 and 51 hours with case *Wind and solar*. The variation in the optimum storage size is also decreased with the addition of solar power.

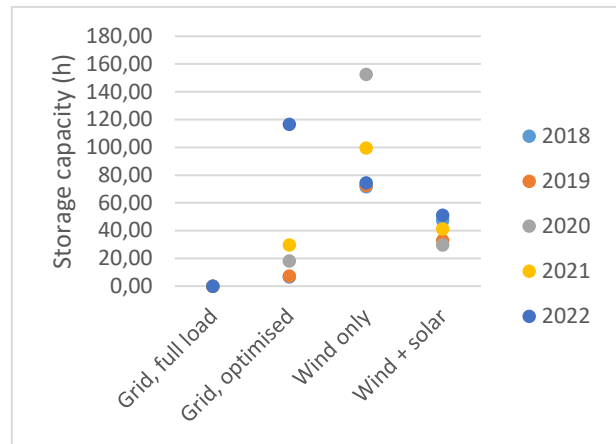
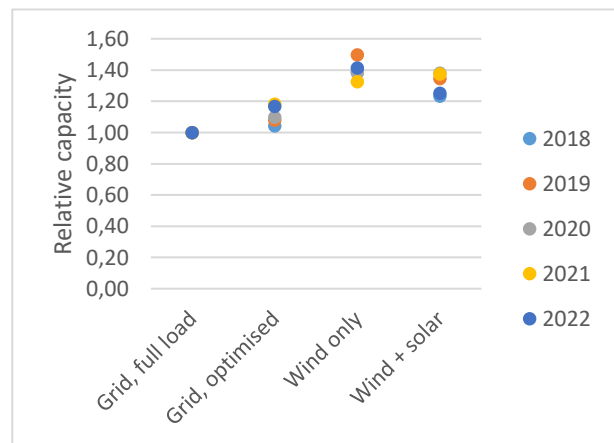


**Figure 7.** Hydrogen storage capacity relative to the electrolyser capacity. 1,0 equals to a storage that can store 1 hour of hydrogen production on full electrolyser power.

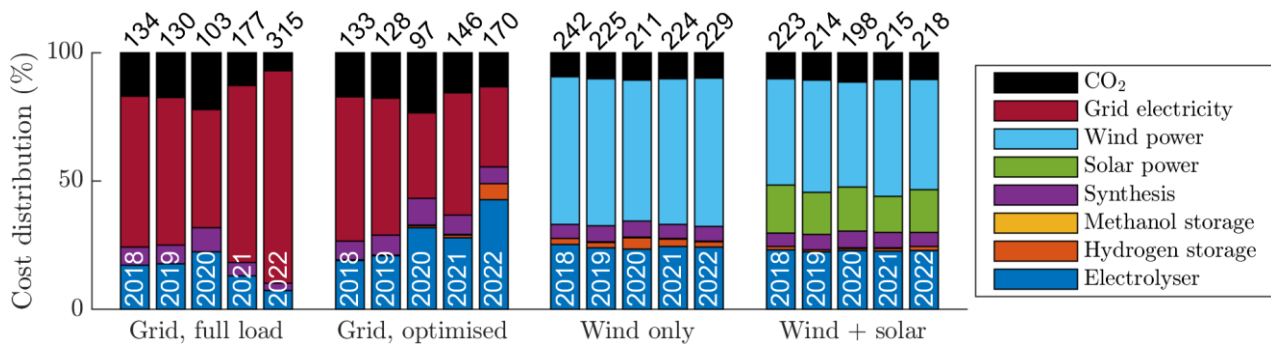
The relative optimum methanol synthesis capacity is illustrated in Figure 8. Relative synthesis capacity is calculated by dividing the optimized synthesis capacity with the capacity in *grid, full load* case, where the synthesis capacity was 100 MW of methanol.

Figure 8 shows that there is less variation in the synthesis optimum capacity than with the electrolyser optimum capacity. *Grid, optimised* case shows very little variation in the optimum capacity, ranging from 1.04 to 1.18. The increasing price volatility has smaller effect on the relative methanol synthesis size than for the relative electrolyser size. During years 2018 - 2022 the synthesis relative size only increased from 1,04 to 1,17. Therefore it can be concluded that the key flexibility in the modelled system originates from the electrolyser, and while the methanol synthesis also has the option to operate on part load, this flexibility is utilized less.

Highest synthesis capacities are seen with case *wind only*, where the relative capacity is between 1,33 and 1,50. Adding solar power to the system decreases the relative synthesis capacity slightly.



**Figure 8.** Relative methanol synthesis plant optimum capacity. Case 1 = 1,0.



**Figure 9.** Relative annual costs. Total annual cost shown above each bar (in millions of euros).

The selected technical parameters allowed synthesis to operate with 50 % power, while electrolyser had no minimum load restriction. To be precise, this assumption is not completely correct – Schmidt et al. states that the minimum part load for alkaline electrolysers is between 10 and 40 % [24]. On the other hand, with large electrolysers consisting of several stacks, some stacks can be put to standby state to allow for larger operation range. However the shutdown of electrolyser stacks can cause a shutdown penalty, that was not considered in this study. The technical parameters of the hydrogen electrolysers are crucial for the results because it is the key process in converting electrical energy into chemical energy.

### 3.3 Cost Distribution

The division of the total annual costs is illustrated in Figure 9. For years 2021 and 2022 in *grid, optimized* case the over dimensioning of the system is considerable compared to the *grid, full load* case and this is visible by the increasing proportion of electrolyser capex and opex cost. The over dimensioning decreases the proportion of grid electricity cost, as electrolyser operation is focused on low-cost hours. Results also show how case *Grid, optimized* always has lower annual costs than the case *Grid, full load*. However, for the years 2018 – 2020 the effect is small and becomes more significant for 2021 and 2022.

The capex of VRE is the largest portion of costs for VRE cases – on average 58 % of annual costs for *wind only* case, and 59 % for the *wind and solar* case.

### 3.4 VRE Capacities and Curtailment

The relative optimum VRE capacity is plotted in Figure 10. Capacity is calculated relative to the electrolyser electrical capacity. The figure shows how adding solar power to the system further increases the over dimensioning of the VRE capacity compared to the electrolyser size. The *Wind only* case has a dimensioning factor of 1,66 to 1,75, and with *Wind and solar* the total VRE dimensioning factor is 2,97 to 3,18. However due to the lower full load hours and investment costs of solar power, the result is logical. When solar power is added to

the system, the wind power capacity is slightly reduced to 1,31 – 1,43 times the electrolyser electrical power.

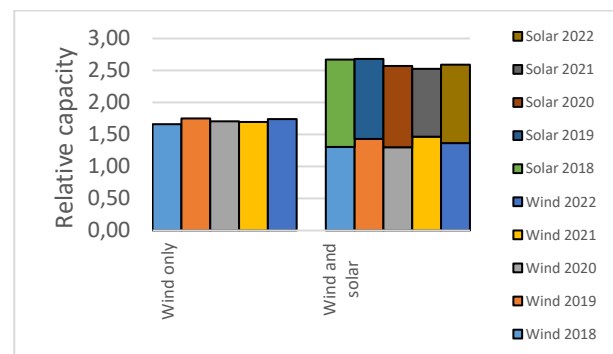


**Figure 10.** VRE capacity relative to the electrolyser capacity.

The curtailment of VRE production is shown in Figure 11. Adding solar power to the system clearly decreases the average curtailment from 11,0 % to 7,7 %. This effect is likely due to the timely distribution of wind and solar power production, and how they complement each other.

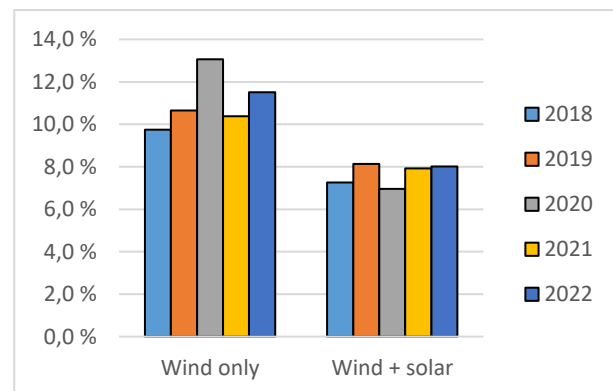


**Figure 11.** Curtailment percentage of VRE.



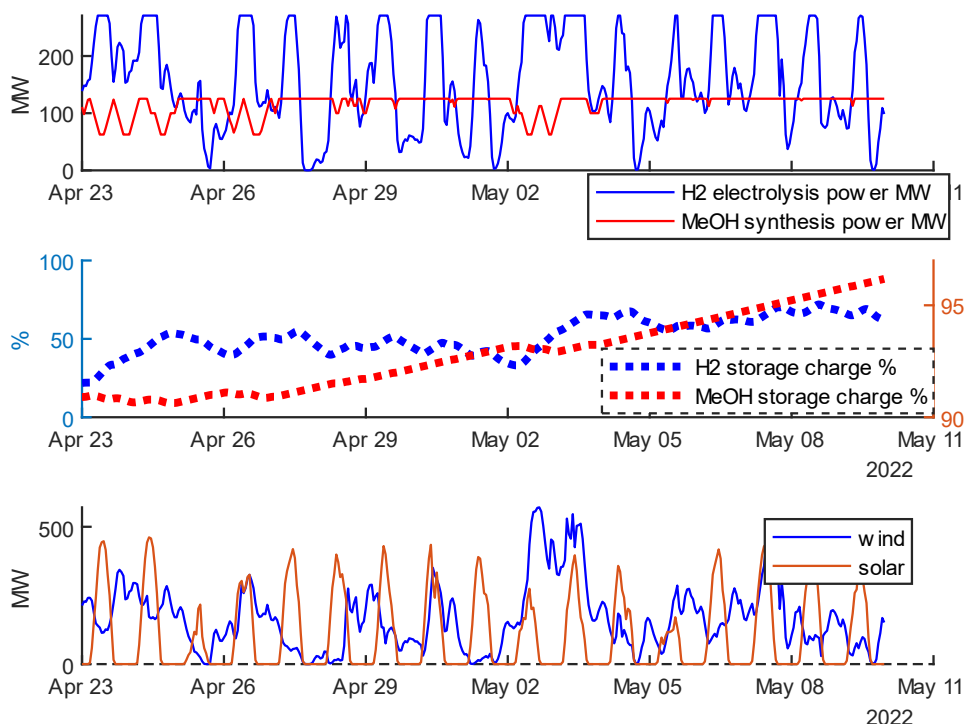


**Figure 12.** Example of the operation of electrolyser, synthesis and the storages during April-May 2022. Case 4, *Wind and solar*

Figure 12 illustrates an example of the e-methanol plant operation during April-May 2022 for case *Wind and solar*. As the plot shows, electrolyser operation is strongly coupled to the VRE production, as there is no storage for electricity. The curtailment of VRE is visible from the flat peaks of the electrolyser power – the electrolyser capacity is smaller than the VRE production peak capacity. The synthesis is decoupled from both the methanol demand and hydrogen production by the buffer storages for H<sub>2</sub> and methanol. Therefore the synthesis operates rather independently, and the part load operation periods in this example do not show strong correlation to other parameters. However in this example the methanol storage is approaching 100% charge, so the part load operation is probably related to limiting the storage charge.

#### 4. CONCLUSIONS

In conclusion, the techno-economic assessment of the e-methanol plant, considering various electricity supply options, has yielded insightful results. The calculated levelized cost of methanol, ranging from 614 €/ton to 1990 €/ton, underscores the significance of both the electricity source and operation strategy.

While VRE cases showed a higher levelized cost of e-methanol compared to spot-priced grid electricity, the optimal plant dimensioning showed reduced year-to-year variation. For VRE cases the levelized cost was between 1246 €/ton and 1530 €/ton. Utilizing both solar and wind power decreased the e-methanol cost by 4 – 8 % compared to using only wind power and this decrease

was attributed to a reduction in VRE curtailment and hydrogen storage sizing.

These findings offer valuable insights into the planning of e-methanol production plants, highlighting emerging possibilities with the fluctuating grid electricity prices. Notably, allowing flexible operation of the e-methanol plant may yield a substantial 46% reduction in production costs, although also necessitating significant changes in plant dimensioning.

Moreover, the system-level benefits are crucial. The flexible operation of the electrolyser and e-methanol production not only can enhance the economic viability of the P2X operator, but also benefits the electricity grid by providing flexible demand. This flexibility can play a pivotal role in balancing the fluctuations of variable renewable energy (VRE) production in the grid, contributing to the stability and sustainability of the energy system.

#### ACKNOWLEDGMENTS

The authors gratefully acknowledge the public financing of Business Finland for the ‘BioCCU’ project. (<https://clicinnovation.fi/project/bioccu/>)

#### REFERENCES

- [1] C. Hank *et al.*, “Economics & carbon dioxide avoidance cost of methanol production based on renewable hydrogen and recycled carbon dioxide-power-to-methanol,” *Sustain Energy Fuels*, vol. 2,

- no. 6, pp. 1244–1261, 2018, doi: 10.1039/c8se00032h.
- [2] S. Sollai, A. Porcu, V. Tola, F. Ferrara, and A. Pettinau, “Renewable methanol production from green hydrogen and captured CO<sub>2</sub>: A techno-economic assessment,” *Journal of CO<sub>2</sub> Utilization*, vol. 68, p. 102345, Feb. 2023, doi: 10.1016/j.jcou.2022.102345.
- [3] IRENA AND METHANOL INSTITUTE, “Innovation Outlook : Renewable Methanol,” 2021. Accessed: Dec. 14, 2023. [Online]. Available: [https://www.irena.org/-/media/Files/IRENA/Agency/%20Publication/2021/Jan/IRENA\\_Innovation\\_Renewable\\_Methanol\\_2021.pdf](https://www.irena.org/-/media/Files/IRENA/Agency/%20Publication/2021/Jan/IRENA_Innovation_Renewable_Methanol_2021.pdf)
- [4] Y. Zheng, S. You, X. Li, H. W. Bindner, and M. Münster, “Data-driven robust optimization for optimal scheduling of power to methanol,” *Energy Convers Manag*, vol. 256, p. 115338, Mar. 2022, doi: 10.1016/j.enconman.2022.115338.
- [5] S. Pfenninger and B. Pickering, “Calliope: a multi-scale energy systems modelling framework,” *J Open Source Softw*, vol. 3, no. 29, p. 825, Sep. 2018, doi: 10.21105/joss.00825.
- [6] J. Forrest and R. Lougee-Heimer, “CBC User’s Guide.” Accessed: Sep. 14, 2023. [Online]. Available: <https://coin-or.github.io/Cbc/>
- [7] “Calliope: A multi-scale energy systems modelling framework,” v0.6.10 Documentation . Accessed: Nov. 20, 2023. [Online]. Available: <https://calliope.readthedocs.io/en/stable/index.html>
- [8] EU Science Hub, “Photovoltaic Geographical Information System (PVGIS).” Accessed: Sep. 14, 2023. [Online]. Available: [https://joint-research-centre.ec.europa.eu/photovoltaic-geographical-information-system-pvgis\\_en](https://joint-research-centre.ec.europa.eu/photovoltaic-geographical-information-system-pvgis_en)
- [9] Copernicus Climate Change Service (C3S) Data Store (CDS)., “Complete ERA5 global atmospheric reanalysis.”
- [10] H. Hersbach *et al.*, “The ERA5 global reanalysis,” *Quarterly Journal of the Royal Meteorological Society*, vol. 146, no. 730, pp. 1999–2049, Jul. 2020, doi: 10.1002/qj.3803.
- [11] Sandia National Laboratories, “PVPerformance Modeling Collaborative.” Accessed: Dec. 14, 2023. [Online]. Available: <http://pvpmc.sandia.gov/>
- [12] N. Martin and J. M. Ruiz, “Calculation of the PV modules angular losses under field conditions by means of an analytical model,” *Solar Energy Materials and Solar Cells*, vol. 70, no. 1, pp. 25–38, Dec. 2001, doi: 10.1016/S0927-0248(00)00408-6.
- [13] R. Urraca, T. Huld, A. V. Lindfors, A. Riihelä, F. J. Martinez-de-Pison, and A. Sanz-Garcia, “Quantifying the amplified bias of PV system simulations due to uncertainties in solar radiation estimates,” *Solar Energy*, vol. 176, pp. 663–677, Dec. 2018, doi: 10.1016/j.solener.2018.10.065.
- [14] T. Huld, R. Gottschalg, H. G. Beyer, and M. Topič, “Mapping the performance of PV modules, effects of module type and data averaging,” *Solar Energy*, vol. 84, no. 2, pp. 324–338, Feb. 2010, doi: 10.1016/j.solener.2009.12.002.
- [15] M. Koehl, M. Heck, S. Wiesmeier, and J. Wirth, “Modeling of the nominal operating cell temperature based on outdoor weathering,” *Solar Energy Materials and Solar Cells*, vol. 95, no. 7, pp. 1638–1646, Jul. 2011, doi: 10.1016/j.solmat.2011.01.020.
- [16] J. Ramon, L. Lledó, V. Torralba, A. Soret, and F. J. Doblas-Reyes, “What global reanalysis best represents near-surface winds?,” *Quarterly Journal of the Royal Meteorological Society*, vol. 145, no. 724, pp. 3236–3251, Oct. 2019, doi: 10.1002/qj.3616.
- [17] S. K. V. S. Sakuru and M. V. Ramana, “Wind power potential over India using the ERA5 reanalysis,” *Sustainable Energy Technologies and Assessments*, vol. 56, p.

- 103038, Mar. 2023, doi:  
10.1016/j.seta.2023.103038.
- [18] J. Olauson, “ERA5: The new champion of wind power modelling?,” *Renew Energy*, vol. 126, pp. 322–331, Oct. 2018, doi: 10.1016/j.renene.2018.03.056.
- [19] A. P. Schaffarczyk, Ed., *Wind Power Technology*. Cham: Springer International Publishing, 2023. doi: 10.1007/978-3-031-20332-9.
- [20] S. Haas *et al.*, “wind-python/windpowerlib: Silent Improvements.” Zenodo, 2021. [Online]. Available: <https://zenodo.org/record/4591809>
- [21] European Network of Transmission System Operators for Electricity, “ENSTO-E Transparency Platform.” Accessed: Sep. 21, 2023. [Online]. Available: <https://transparency.entsoe.eu/>
- [22] International Renewable Energy Agency, *Renewable power generation costs in 2021*. 2022. [Online]. Available: [www.irena.org](http://www.irena.org)
- [23] European Commission, Directorate-General for Energy, J. Cihlar, A. Villar Lejarreta, and A. Wang, “Hydrogen generation in Europe: Overview of costs and key benefits,” *EU Publications Office*, 2021.
- [24] O. Schmidt, A. Gambhir, I. Staffell, A. Hawkes, J. Nelson, and S. Few, “Future cost and performance of water electrolysis: An expert elicitation study,” *Int J Hydrogen Energy*, vol. 42, no. 52, pp. 30470–30492, Dec. 2017, doi: 10.1016/j.ijhydene.2017.10.045.
- [25] Ovako Press Release, “ Fossil-free hydrogen initiative by Ovako, Volvo Group, Hitachi ABB Power Grids Sweden, H2 Green Steel and Nel Hydrogen.” Accessed: Sep. 15, 2023. [Online]. Available: <https://www.ovako.com/en/newsevents/news--press-releases/ovako-press-release-detail/?releaseId=B4ADD5355036AA5F>
- [26] D. D. Papadias and R. K. Ahluwalia, “Bulk storage of hydrogen,” *Int J Hydrogen*
- Energy*, vol. 46, no. 70, pp. 34527–34541, Oct. 2021, doi: 10.1016/j.ijhydene.2021.08.028.

**Open Access** This chapter is licensed under the terms of the Creative Commons Attribution-NonCommercial 4.0 International License (<http://creativecommons.org/licenses/by-nc/4.0/>), which permits any noncommercial use, sharing, adaptation, distribution and reproduction in any medium or format, as long as you give appropriate credit to the original author(s) and the source, provide a link to the Creative Commons license and indicate if changes were made.

The images or other third party material in this chapter are included in the chapter's Creative Commons license, unless indicated otherwise in a credit line to the material. If material is not included in the chapter's Creative Commons license and your intended use is not permitted by statutory regulation or exceeds the permitted use, you will need to obtain permission directly from the copyright holder.

